Arab Remote Sensing and Geographic Information System Organisation

Hyperspectral Indices For Assessing Damage By The Red Palm Weevil Rhynchophorus Ferrugineus (Coleoptera: Curculionidae) In Date Palms

Yones, M. S.; Aboelghar, M. A.;El-Shirbeny, M. A.; Khdry, G.A.; Ali, A. M.; Saleh, N.S.
National Authority for Remote sensing and Space Sciences (NARSS).

KEYWORDS: Remote sensing, hyperspectral data, red palm weevil (RPW), date palms, monitoring, predictions

ABSTRACT

The red palm weevil (RPW), Rhynchophorus ferrugineus (Olivier) (Coleoptera: Curculionidae) is a highly destructive pest of date palms, Phoenix dactylifera in several countries. The RPW larvae bore deep into palm crowns, trunks and offshoots, concealed from visual inspection until the palms are nearly dead. Traded palm trees are intensively transported between and within countries, spreading the pest worldwide. Consequently, an urgent need exists to identify and monitor concealed RPW larvae. Monitoring of this pest is generally error prone. Alternately, radiometry is a reliable technique for rapid and non-destructive assessment of plant health. The purpose of this research was to develop a mathematical method to automatically detect infested palm plant with RPW. A study was conducted to characterize reflectance spectra of palm plants with known red palm weevil infestation levels (grade-0 is healthy and grade-2 is severe), and seek to identify specific narrow wavelengths sensitive to RPW damage. Reflectance measurements were made in the spectral range of 350–2500 nm using a hyperspectral radiometer. Reflectance sensitivity analysis of the hyperspectral data to RPW damage also determined. Results of this study could suggest potential usage of remote sensing in monitoring spatial distribution of the RPW, and thereby enable effective planning and implementation of site-specific pest management practices. The study shows that it is feasible to detect RPW infestation using the hyperspectral data and recognize its level, which could be utilized to monitor trade and predictions.

INTRODUCTION

A red palm weevil, *Rhynchophorus ferrugineus* (RPW), is a key pest of horticultural and ornamental palm species in Asia, the Middle East and the Mediterranean region. The RPW is currently spreading in Mediterranean European countries, endangering picturesque landscapes that are very attractive to tourists (**Soroker et al., 2005, 2006 and Khalid, 2007**). The female RPW lays eggs in injuries in the trunks of established trees, at the base of the palm leaves, at tree crowns and adjacent to offshoots. The RPW larvae bore deep into palm crowns, trunks, and offshoots, generally concealed from visual inspection until the palms are nearly dead. Several weevil generations may develop within a single tree. Infested trees suffer from reduced productivity. Heavy infestations often result in collapsed trees and thus, total loss of crops (**Blumberg et al., 2001**). Young palm trees (and in the case of date palms, their offshoots) are intensively traded and transported between and within countries, therefore the pest is spread worldwide (**Giblin-Davis, 2001**). Quick predictions and control timing act as a valuable tools used in an integrated control program for managing Pests in Egypt also the early prediction of insects to help the farmers to avoid heavy sprays of pesticides and take the necessary actions to restrict dangerous infestations (**Yones et al., 2012**).

Remote sensing is the science and art of obtaining information about an object, area, or phenomenon through the analysis of data acquired by a device that is not in contact with the object under investigation (**Lillesand et al., 2004**). The advancements of sensor technology and growing operational deployment of ground-based, airborne and space-borne instruments greatly enhance the capabilities for routinely acquiring hyperspectral data and potentially quantifying plant pigments over a wide range of spatial and spectral scales (**Blackburn, 2007**). The use of remote sensing for detection of crop pests and diseases is based on the assumption that stresses induced by them interferes with photosynthesis and physical structure of the plant, and affects the absorption of light energy, thus altering the reflectance characteristics of the plants

(**Hatfield and Pinter, 1993**). Recent developments in optical technology have made it possible to differentiate diseased and healthy crops, and thus the prospect of automatically measuring the spatial distribution of crop diseases and insect pests. Spectroscopic and imaging techniques could be integrated with an autonomous agricultural vehicle that can provide information on early detection of disease and spatial distribution, thereby provide spatially selective sprays for pesticide application (**West et al., 2003**). Remote sensing can create geo-referenced stratified maps of fields with pest abundance and damage without a large number of samples and provide spatial approaches for pest control (**Willers et al., 2005; Voss et al., 2010; Karimzadeh et al., 2011; Dammer and Adamek, 2012; Mirik et al., 2012**). At the same time, hyperspectral remote sensing could be used to identify the spectral signature of each object. Spectral signature is the specific combination of reflected and absorbed electromagnetic radiation at varying wavelengths which can uniquely identify an object (**Aboelghar and Abdel Wahab, 2013**).

The main objective was to identify the best spectral zone as the first step and the optimal waveband as the second step to discriminate between date palms (healthy, moderate and severely infected) and the palm offshoots (healthy and infected), for early prediction of pest infestation and helping for encourage the integrated pest management system.

1. STUDY AREA

The study Area covers an area of about 14.961.7 m² in the North part of Nile Wadi and the Middle part of Egypt in the Eastern flood plain. It is located in the southern part of Giza governorate Figure (1). It is bordered from the north by El Saff and Helwan City and Masjid Mousa and El Korimaate from the South, and the river Nile from the east and El Mazaa Gabel and Eastern desert From the East. It's located between latitudes 29º 22' 41.804" and 29º 22' 34.34" North and between longitudes 31º 15' 13.11" and 31º 15" 15.249" East. The climatic is arid to semi arid reflecting the typical climate of the Nile Delta, The topography of the area is nearly flat except for the areas occupied by Vertic Torrifluvents.

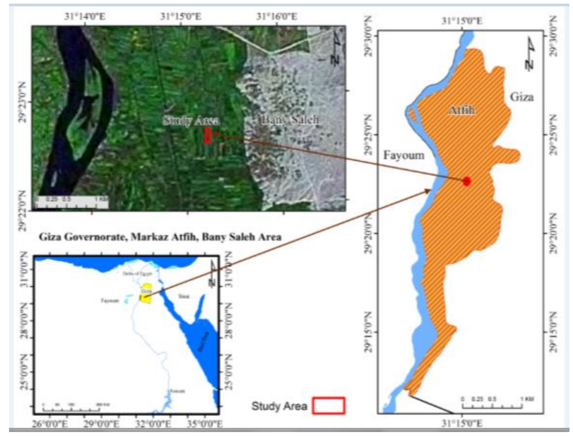

Figure1: Location of the study area (Giza governorate).

2. MATERIAL AND METHODS

The methodology of this work focused on field hyperspectral measurements and statistical analysis for the output measurements in order to choose the optimal spectral and then the optimal waveband/s inside each spectral zone that can be used to zone to detect infested palm plant with RPW. As the final objective of this work is presenting information that could be used to increase the accuracy and performance of the existing remote sensing software's in identify the different grades in the palm infestation. The full description of the used methodology is explained in the following subsections.

2.1. Field hyper spectral measurements

Analytical field spectroradiometer (ASD Field Spec) was used to measure the reflection of the different date palms under investigation. Data were collected on cloudless days from 10 am clock to 2 pm clock in order to minimize external effects from the atmospheric conditions and changes in solar position. The average of twenty leaves along the study area for each palm was calculated to be used in the study. Measurements were carried out in a full optical spectral range (Visible – Near Infrared – Short Wave Infrared) starting from 350 nm to 2500 nm with 1 nm interval output data. The sampling interval is 1.4 nm at the spectral range (350-1050 nm) while it is 2 nm at the spectral range (1000-2500 nm). These are the intervals which the device is capturing the reflectance. The device automatically performs an interpolation for the data and gives the final data output with (1 nm) interval for the all spectrum range (350-2500 nm). The spectrum characteristics of the device are shown in Table 1. The protocol used for the collection of spectral data is based on measuring radiance from a Spectralon® panel. A designed probe was attached to the instrument's fiber-optic cable to be used to ensure standardized environmental conditions for reflectance measurement. The fiber-optic cable provides the flexibility to adapt the instrument to a wide range of applications. Bare foreoptic 25 degrees used for outdoor measurements resulting circular field of view with 3 cm diameter as measurements were taken at 5 cm height in nadir position (90 degrees) over the measured plants. In the current study, the measurements were performed by holding the pistol grip by hand. As recommended in the instructions of using the device, the Spectralon® was tilted directly towards the sun during optimization. Data were collected on cloudless days from 10 am clock to 2 pm clock in order to minimize external effects from the atmospheric conditions and changes in solar position. Immediately after the white standard radiance measurement, five spectra of the canopy were obtained. Each one of them is the average of 20 reading. All of the measurements were made with the sensor located directly over the center of the canopy. The mean of the five spectra was then determined to provide a single spectral value.

Spectral Range	350-2500 nm
Spectral Resolution	3 nm : 700 nm 8.5 nm : 1400 nm 6.5 nm : 2100 nm
Sampling Interval	1.4 nm : 350-1050 nm 2 nm : 1000-2500 nm

Table 1: The ASD Field Spec 3 Specifications

2.2 One Way ANOVA and Tukey's HSD Post Hoc Analysis.

Spectral zones that represent the atmospheric windows (portions of the electromagnetic reflectance that include data noise because of the relative air humidity) were removed. Spectral pattern of each measured sample was identified. Generally, spectral reflectance could be divided into six different spectral portions as follows: blue (350 - 440 nm), green (450 - 540 nm), red (550 - 750 nm), NIR (760 - 1000 nm), SWIR I (1010–1775 nm) and SWIR II (2055–2315 nm).

2.2.1: Comparing Standard Deviations from Several Populations

Analysis of variance (ANOVA) methods are presented for comparing means from several populations or processes. While similar methods are occasionally used for comparing several standard deviations, often using the natural logarithm of sample variances as the response variable, they are not a main focal point of this work. There are also a number of alternative procedures that are not based on ANOVA methods that can be used to com- pare standard deviations. Two of these are described be- low. Both are highly sensitive to departures from the assumption of normality; consequently, they should be used only after verification that the assumption of normally distributed errors is reasonable. When using ANOVA models with data from designed experiments, a valuable assessment of the assumption of constant standard deviations across k factor-level combinations is given by the $F_{\max}$ test The $F_{\max}$ test is used to test the hypotheses (**Mason et al., 2003**) (Equation (1)).

$$F_{Max} = \left(\frac{\max(s_i)}{\min(s_i)}\right)^2 \quad (1)$$

2.2.2: Multiple Comparisons

The *F*-statistics in an ANOVA table provide the primary source of information on statistically significant factor effects. However, after an *F*-test in an ANOVA table has shown significance, an experiment usually desires to conduct further analyses to determine which pairs or groups of means are significantly different from one another (**Mason et al., 2003**).

2.2.3: Tukey's Significant Difference Procedure

Tukey's procedure controls the experiment wise error rate for multiple comparisons when all averages are based on the same number of observations. The stated experiment wise error rate is very close to the correct value even when the sample sizes are not equal. The technique is similar to Fisher's LSD procedure. It differs in that the critical value used in the TSD formula is the upper 100*α*% point for the difference between the largest and smallest of *k* averages. This difference is the range of the *k* averages, and the critical point is obtained from the distribution of the range statistic, not from the *t*-distribution (Equation (2)).

2.2.4: Two averages *and*, based on and observations respectively, are significantly different if:

$$|\bar{y}_i - \bar{y}_j| > TSD$$

Where

$$TSD = q(\alpha; k, v)\left(MS_E \frac{n_i^{-1} + n_j^{-1}}{2}\right)^{\frac{1}{2}} \tag{2}$$

2.3Linear Discriminate Analysis

Linear Discriminate Analysis (LDA) is a method to discriminate between two or more groups of samples. The groups to be discriminated can be defined either naturally by the problem under investigation, or by some preceding analysis, such as a cluster analysis. The number of groups is not restricted to two, although the discrimination between two groups is the most common approach. Linear Discrimination Analysis (LDA) is a commonly used technique for data classification. LDA approach is explained by **Axler, 1995**. It easily handles the case where the within-class frequencies are unequal and their performance has been examined on randomly generated test data. This method maximizes the ratio of between-class variance to the within-class variance in any particular data set thereby guaranteeing maximal separation. LDA doesn't change the location but only tries to provide more class separation and draw a decision region between the given classes. This method also helps to better understand the distribution of the feature data. In the current study, Class-independent transformation type of LDA was performed. This approach involves maximizing the ratio of overall variance to within class variance. It uses only one optimizing criterion to transform the data sets and hence all data points irrespective of their class identity are transformed using this transform. In this type of LDA, each class is considered as a separate class against other classes. In LDA, within-class and between class scatter are used to formulate criteria for class separation. Within-class scatter is the expected covariance of each of the classes. The scatter measures are computed using Equations (3) and (4).

$$Sw = \sum_j Pj \times (\mathrm{cov}_j) \tag{3}$$

Therefore, for the two-class problem,

$$Sw = 0.5 \times \mathrm{cov}_1 + 0.5 \times \mathrm{cov}_2 \tag{4}$$

All the covariance matrices are symmetric. Let and be the covariance of set 1 and set 2 respectively.
Covariance matrix is computed using the following equation (5).

$$\mathrm{cov}\ j = \left(x_j - \mu_j\right)\left(x_j - \mu_j\right)^T \tag{5}$$

Then, the between-class scatter is computes using the following equation (6).

$$Sb = \sum_j (\mu_j - \mu_3) \times (\mu_j - \mu_3)^T \tag{6}$$

Sb can be thought of as the covariance of data set whose members are the mean vectors of each class. As defined earlier, the optimizing criterion in LDA is the ratio of between-class scatter to the within-class scatter. The solution obtained by maximizing this criterion defines the axes of the transformed space. As LDA is a class independent type in this study, the optimizing criterion is computed as equation (7)

$$criterion = inv(sw) \times Sb \tag{7}$$

Finally, transforming the entire data set to one axis provides definite boundaries to classify the data. The decision region in the transformed space is a solid line separating the transformed data sets thus equation (8)

$$transforme\_set = transform\_spec^T \times data\_set^T$$
(8)

This analysis was carried out twice to discriminate between Healthy, infected and severely infected palms and again healthy and infected palm offshoots.

3. RESULTS AND DISCUSSION

Spectral reflectance pattern for the three date palms with its different degrees of infestation is shown in Figure 2. Reflectance pattern showed the same trend for the three palms; however, reflectance of the Healthy palm (grade 0) was higher than reflectance of the moderately infected palm (grade1) while the reflectance of severely infected palm (grade 2) is the lowest at the whole spectrum. Comparing the reflectance in the different spectral zones for the three palms showed that the highest spectral reflectance was in infrared spectral zone (700–1300 nm), relatively low reflectance in the spectral zone (1450–1800 nm) while the lowest reflectance was found in the spectral zone (1950-2300 nm). In case of palm offshoots the spectral reflectance pattern as shown in Figure 3 showed the same trend and also the spectral reflectance of Healthy offshoots was higher than the reflectance of infected ones.

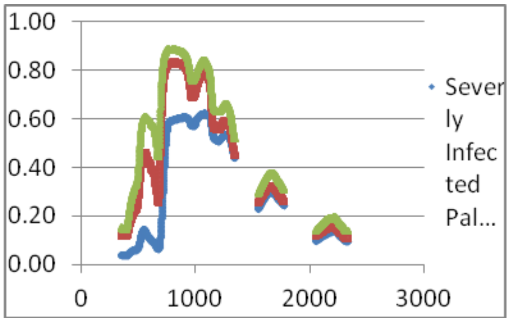

Figure 2: The Spectral Reflectance Pattern for Palms with different Grade of infestation (healthy, moderate and severely infected).

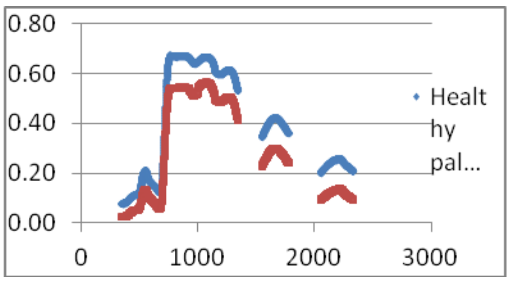

Figure 3: The Spectral Reflectance Pattern for Healthy and infected Palm Offshoots.

The reason of this might be due to the effect of pest infestation to the date palm which make loses to the essential elements in the palm leaves. The results of Tukey's HSD test showed the significance of the spectral difference between Healthy and infected palm along the six spectral zones attached with the general mean of the reflectance for them, the mean of the reflectance for each one, the maximum and minimum reflectance values for each palm. The significance of the difference between healthy, moderately and severely infected palm also appears in each figure. Tukey's HSD test showed that only Red spectral zone is the best to differentiate between healthy, moderately and severely infected palms followed by blue, green, NIR and SWIR-2 spectral zones that showed relatively high potentiality to differentiate between them. At the same time, SWIR-1 spectral zone did not show significant difference in the reflectance of Healthy, moderately and severely infected palms as shown in Figure 4.

For the discrimination between healthy and infected palm offshoots, the six spectral zones were sufficient to classify the two palms as explained in Figure 3. SWIR -2 and blue showed the best result to discriminate between healthy and infected palm offshoots. Red, green, NIR and SWIR-2 spectral zones shows acceptable results, but SWIR-1 spectral zone did not show remarkable significant difference as shown in Figure 5.

The process of this work included applying two statistical analyses on the spectral measurements of the field spectroradiometer. The main objective was to identify the best spectral zone as the first step and the optimal waveband as the second step to discriminate between date palms (healthy, moderate and severely infected) and the palm offshoots (healthy and infected). The final objective is to improve the performance of the existing remote sensing software's in early detection of palm infestation through machine learning process. Comparing the spectral reflectance pattern for the three date palms (healthy, moderate and severely infected) and palm offshoots (healthy and infected) showed high spectral similarity between them.

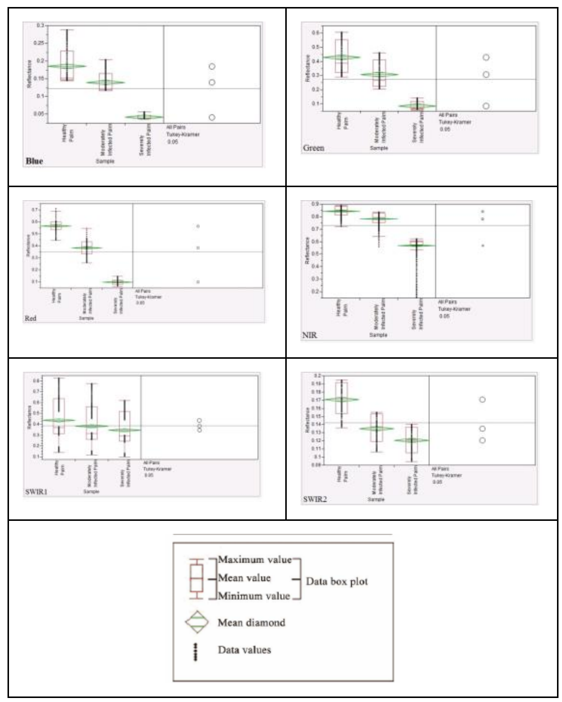

Figure 4: ANOVA and Tukey's HSD analysis to differentiate between palm (healthy, moderate and severely infected) and the palm offfshots (healthy and infected).

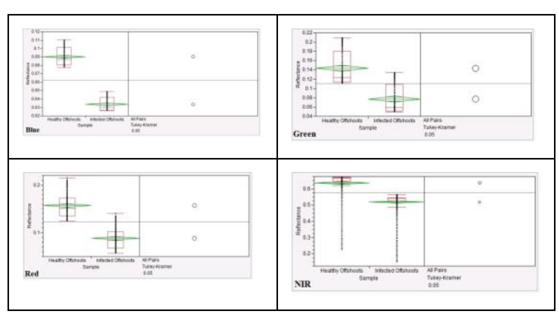

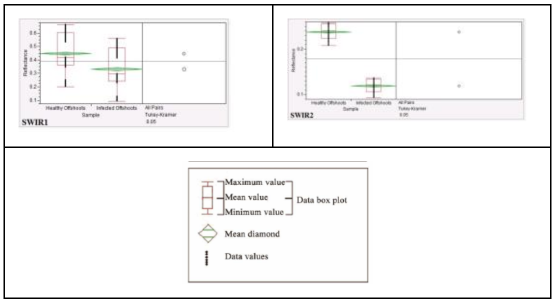

Figure 5: ANOVA and Tukey's HSD analysis to differentiate between the palm offshoots (healthy and infected).

The results of the statistical analysis explained that red spectral zone is the best spectral zones to differentiate between date palms (healthy, moderate and severely infected) while blue and SWIR-2 spectral zones are the best spectral zones to differentiate between palm offshoots (healthy and infected) as show in figure 4 and 5. Only one specific waveband zone, (720:724 nm) in the case of Severely Infected Palm, was found the best to isolate from Healthy and moderately infected palm. At the same time, three spectral wavebands were sufficient to isolate Moderately infected palm (529:589, 693:695, 693:695 nm) while two spectral wavebands were sufficient to isolate Healthy Palm (514:664, 684:1344 nm). In case of palm offshoots there is two spectral wavebands were sufficient to isolate infected offshoots with remarkable two waveband for infection is (1551:1779 , 2051:2334 nm) from Healthy offshoots (720:724, 1566:1778 nm) as illustrated in table 2. All measurements were carried out on Siwa date palms of the same age, 15 years old.

Although the moderately infected samples were characterized through three unique spectral zones, this result is quite important as remote sensing data could be used for the early warning of moderately and slightly infected palms. This is considered the key point used in integrated pest management system.

	Optimal wavelength zones (nm)
Healthy Palm	514-664
	684-1344
Moderately Infected Palm	529-589
	693-695
	1333-1335
Severely Infected Palm	720-724
Healthy Offshoots	715-720
	1566-1778
Infected Offshoots	350-718
	1551-1779
	2051-2334

Table 2: The optimal waveband to differentiate between (healthy, moderately and severely infected) date palms or offshoots.

4. CONCLUSION

Spectral libraries collected in the field are common data sets exploited by the hyperspectral remote sensing community. Such data support the analysis of airborne and space borne hyperspectral imagery, the characterization of natural material, and the development of algorithms for information extraction (Rivard et al., 2008). So the integration of remote sensing and GIS techniques for the integrated pest management programs is essential. Field hyper spectral measurements were used to discriminate between date palms (healthy, moderate and severely infected) and palm offshoots (healthy and infected). Two steps of statistical analysis showed the best spectral zone and the optimal wavebands to discriminate between them. Tukey's HSD test indicated that SWIR-2 spectral zone was the best while SWIR-1 was the worst for the discrimination between date palms (healthy, moderate and severely infected) and palm offshoots (healthy and infected). The other spectral zones showed also acceptable results for differentiation. Linear discrimination analysis showed specific wavebands to identify infected palm dates from the healthy one. It was found that the only one specific waveband zone, (720:724 nm) in the case of Severely Infected Palm, was found the best to isolate from Healthy and moderately infected palm. At the same time, three spectral wavebands were sufficient to isolate Moderately infected palm (529:589, 693:695, 693:695 nm) this result is quite important as remote sensing data could be used for the early warning of moderately and slightly infected palm, this is considered the key point used in integrated pest management system, while there are two spectral wavebands were sufficient to isolate Healthy Palm (514:664, 684:1344 nm). In case of palm offshoots there is two spectral wavebands were sufficient to isolate infected offshoots is (1551:1779, 2051:2334 nm) from Healthy offshoots (720:724, 1566:1778 nm).

5. REFERENCES

Aboelghar, M. and H. Abdel Wahab, Spectral footprint of Botrytis cinerea, a novel way for fungal characterization, Advances in Bioscience and Biotechnology, 4, pp. 374-382, 2013.

Axler, S. , Linear Algebra Done Right, Springer-Verlag New York Inc., New York, New York, 1995.

Blackburn, G.A., Hyperspectral remote sensing of plant pigments, Journal of Experimental Botany 58, pp. 855–867, 2007.

Blumberg, D., A .Navon, E. Kehat, S. Levski, Date palm pests in Israel early second millennium, Alon Hanotea 55, pp. 42–48, 2001.

Dammer, K.H., R. Adamek, Sensor-based insecticide spraying to control cereal aphids and preserve lady beetles, Agronomy Journal 104, pp. 1694–1701, 2012.

Giblin-Davis, R.M., Borers of palms, In: Moore, D., R.M. Giblin-Davis, R.G. Abad, (Eds.), Insects on Palms, Howard CABI Publishing, Wallingford, UK, pp. 267–305, 2001.

Hatfield, J.L., P.J. Pinter, Remote sensing for crop protection, Crop Protection 12, pp. 403–413, 1993.

Karimzadeh, R., M.J. Hejazi, H. Helali, S. Iranipour, S.A. Mohammadi, Assessing the impact of site-specific spraying on control of Eurygaster integriceps (Hemiptera: Scutelleridae) damage and natural enemies, Precision Agriculture 12, pp. 576–593, 2011.

Khalid, A.A., 2007, Red palm weevil home, Available at: www.redpalmweevil.com.

Lillesand, T.M., R.W. Kiefer, J.W. Chipman, Remote Sensing and Image Interpretation. John Wiley & Sons Inc., pp. 763, 2004.

Mason, R. L., R. F. Gunst, and J. L. Hess, Statistical Design and Analysis of Experiments with Applications to Engineering and Science 2nd Edition, (A John Wiley & Sons Publications), 2003.

Mirik, M., R.J. Ansley, Jr. G.J. Michels, N.C. Elliott, Spectral vegetation indices selected for quantifying Russian wheat aphid (Diuraphis noxia) feeding damage in wheat (Triticum aestivum L.), Precision Agriculture 13, pp. 501–516, 2012.

Rivard, B., J. Feng, A. Gallie, S.A. Azofeifa, Continuous wavelets for the improved use of spectral libraries and hyperspectral data, Remote Sensing of Environment 112, pp. 2850–2862, 2008.

Soroker, V., D. Blumberg, A. Haberman, M. Hamburger-Rishard, S. Reneh, T. Salavat, L. Anshelevich, A.R. Harari, The current status of red palm weevil infestation in date palm plantations in Israel, Phytoparasitica 33, pp. 97–106, 2005.

Soroker, V., Gindin, G., Glazer, I., Pinhas, J., Levsky, S., Eliahu, M., Biton, S., Haberman, A., Nakache, Y., Mizrach, A., Hetzroni, A., 2006. The red palm weevil infestation in Israel: occurrence and management. In: I Jornada International sobre el Picudo Rojo de la Palmeras. Agroalimed, Generalitat Valenciana, pp. 59–79, 2005.

Voss, K., J. Franke, T. Mewes, G. Menz, W. Kühbauch, Remote sensing for precision crop protection – a matter of scale, In: Oerke, E.C.; R. Gerhards, G. Menz, R.A Sikora, (Eds.), Precision Crop Protection – the Challenge and Use of Heterogeneity, Springer, Heidelberg, ISBN 978-90-481-9276-2, 2010.

West, J.S., C. Bravo, R. Oberti, D. Lemaire, D. Moshou, H.A. Mc Cartney, The potential of optical canopy measurement for targeted control of field crop diseases, Annual Review of Phytopathology 41, pp. 593–614, 2003.

Willers, J.L., J.N. Jenkins, W.L. Lander, P.D. Gerard, D.L. Boykin, K.B. Hood, P.L. Mckibben, S.A. Samson, M.M. Bethel, Site specific approaches to cotton insect control, sampling and remote sensing analysis techniques, Precision Agriculture 6, pp. 431–452, 2005.

Yones, M. S.; S. M. Arafat; A. F. Abou Hadid; H. A. Abd Elrahman and H. F. Dahi, Determination of the best timing for control application against cotton leaf worm using remote sensing and geographical information techniques, The Egyptian Journal of Remote Sensing and Space Sciences, 15, pp. 151–160, 2012.